



HAL
open science

Localization of Defects in Pipes Using Guided Waves and Synthetic Aperture Focussing Technique (SAFT)

Tobias Gaul, Lars Schubert, Bianca Weihnacht, Bernd Frankenstein

► **To cite this version:**

Tobias Gaul, Lars Schubert, Bianca Weihnacht, Bernd Frankenstein. Localization of Defects in Pipes Using Guided Waves and Synthetic Aperture Focussing Technique (SAFT). EWSHM - 7th European Workshop on Structural Health Monitoring, IFFSTTAR, Inria, Université de Nantes, Jul 2014, Nantes, France. hal-01020390

HAL Id: hal-01020390

<https://inria.hal.science/hal-01020390>

Submitted on 8 Jul 2014

HAL is a multi-disciplinary open access archive for the deposit and dissemination of scientific research documents, whether they are published or not. The documents may come from teaching and research institutions in France or abroad, or from public or private research centers.

L'archive ouverte pluridisciplinaire **HAL**, est destinée au dépôt et à la diffusion de documents scientifiques de niveau recherche, publiés ou non, émanant des établissements d'enseignement et de recherche français ou étrangers, des laboratoires publics ou privés.

LOCALIZATION OF DEFECTS IN PIPES USING GUIDED WAVES AND SYNTHETIC APERTURE FOCUSING TECHNIQUE (SAFT)

Tobias Gaul¹, Lars Schubert¹, Bianca Wehnacht¹, Bernd Frankenstein¹

¹ Fraunhofer Institute for Ceramic Technologies and Systems IKTS -MD (Material Diagnostics),
Maria-Reiche-Str. 2, D-01109 Dresden, Germany

lars.schubert@ikts-md.fraunhofer.de

ABSTRACT

In order to monitor offshore foundations of wind turbines permanently, durable sensors and sensor systems are needed which are well suited for the harsh environmental conditions. Additionally, the restricted offshore repair opportunities and therefore the urgent need for high reliability have to be taken into account. For the monitoring of welded seams in these applications areas, sensor rings were tested and qualified.

The present paper introduces a technique to localize cracks in cylindrical structures as they are used for offshore foundations. The proposed technique is based on the use of elastic waves propagating in hollow cylinders. The so-called guided waves are used in a variety of wave modes. Every wave mode induces a different interaction potential with a crack depending on frequency and elastic stress components. Using the Finite difference method, the time-dependent elastic problem is solved by the simulation software Wave3000Plus to determine well-suited wave modes and frequency domains for the interaction of waves with the expected cracks. Subsequently, measurements using a cylindrical test structure were performed to verify the simulation results. Varying wave modes provide differing main oscillation directions and require the usage of shear transducers and thickness crystal transducers. Furthermore, the synthetic superposition technique is approved by experiments on cracks with varying depth.

KEYWORDS : *Guided waves, Pipe inspection, Imaging technique, SHM*

1. INTRODUCTION

On June 30, 2011, the federal government decided to shut down the nuclear power plants until 2022 and announced the energy turnaround to renewable energies. In the coming years, the number of offshore wind turbines in the Nordic and Baltic Sea will increase rapidly. According to "Windresearch", until Dec. 31, 2010 3.869 MW offshore power was installed in Europe. As announced by the German federal government, the power shall be extended by 10.000 MW only in Germany until 2020. Especially the foundations of the wind turbines are highly stressed by wind, waves and the permanent excitation of the rotation movement. Cyclic loads are interfered in a complex way by stochastic loads. This influences the global stability and the development of local structural changes (welded seam cracks). Both can lead to a complete failure of the structure. All off-shore foundations used today have welded seams which are weak zones due to the thermal material treating and can be regarded as potential sources of cracks. In order to meet the demanded liability needs for the operator in the time range of 20 years, concepts have to be developed to automatically monitor the wind turbine regarding local and global structural changes.

The paper presents a method for localizing fatigue cracks in off-shore foundations. The application of guided waves is a promising alternative to conventional NDT. The waves propagate along the pipe's longitudinal direction with minor damping compared to conventional ultrasonic testing. Because of the longer range, no direct access is necessary in the monitoring area. Sensors are positioned around

the pipe in a ring configuration. One sensor serves as actor, the others as sensors. A sequential recording of all transmitting and recording paths gives numerous time signals for processing. Scattering areas in the monitoring area are reconstructed by synthetic focussing algorithms (SAFT). Experiments in lab scale were downscaled from real application scenarios, whereas in scaled and unscaled cases an equivalent behaviour of the guided waves is generated. Based on the scaled system, simulation based on finite differences algorithms were performed in order to identify suited transducer configurations and wave modes for the damage interaction of guided waves in pipes with cracks. Numerous models are available for selected modes proofed by experiments and numerical applications [1–3]. Finally, the practical proof of the interference is carried out using a demonstrator in labscale. The identified modes from simulations are exited in an applied actor-sensor-ring in the considered frequency range. The introduced crack was detected by synthetic focusing techniques and the results evaluated regarding their quality.

2. MEASUREMENT PRINCIPLE

Guided waves are used which are described in detail in different papers, for example in [1, 4, 5]. The dispersion curve of phase velocity for the selected structure is given in Figure 1. The dashed rectangle highlights the frequency-thickness domain, which was used in all following investigations. The occurring modes are computed as plate modes and labelled as equivalent pipe modes in the therefore mentioned rectangle.

With conventional pitch-catch or pulse-echo arrangement used e.g. by Park [6] or Kim [7] it is possible to localize flaws only in a restricted area. In offshore-applications it is necessary to inspect large areas for integrity. To check a flaw in detail it is essential to know the position of the flaw along the pipe. In this work an adapted SAFT-algorithm for pipes is used which based is on the fundamentals of SAFT-technique applied conventional ultrasonic testing. In contrast to phased array technique, the applying of time delays and summation of time signals is carried out after transmitting and receiving all signals as post-processing. The principle of SAFT is presented in Figure 2. A transducer at point Q_s transmits a wave which is received at the transducer Q_r . Knowing the wave velocity, it is possible to calculate the theoretical arrival time from any backscattered wave at any image point by

$$t_r = \frac{|Q_s - Q_p|}{c} + \frac{|Q_p - Q_r|}{c}. \quad (1)$$

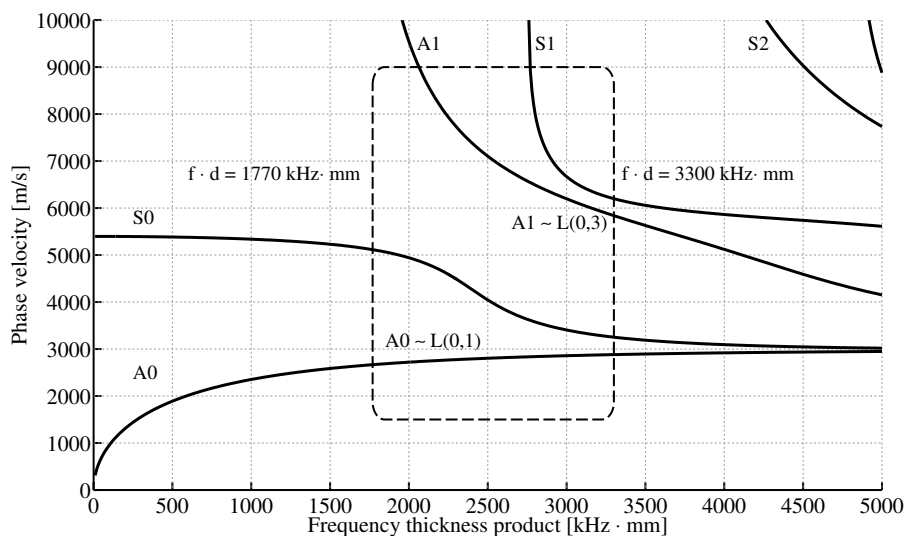


Figure 1 : Lamb wave dispersion curve for phase velocity for S355 mild steel, material parameter shown in section 3.1

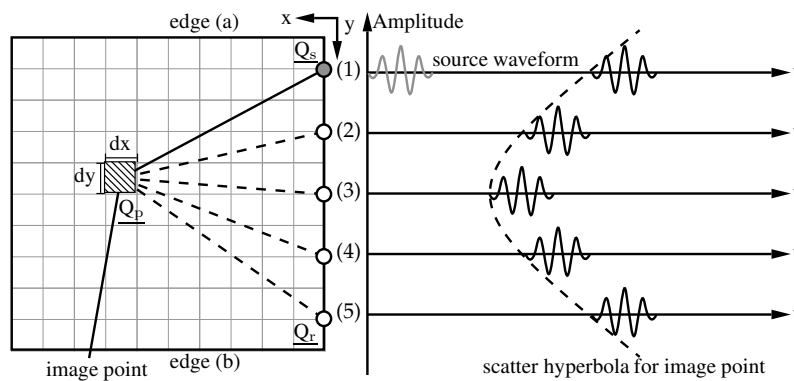


Figure 2 : Principle of SAFT image reconstruction [8]

Any image point refers to a point that describes the hypothetical reflection from a scatter point. All discrete values along these points are summed and define the value of the image point. After instrumentation, a baseline is created by receiving all transmitter-receiver paths. Measurements are repeated in a predefined cycle and the newly received data are compared with baseline data to draw conclusions about the condition of the structure.

The use of SAFT for tubular structures requires additional boundary conditions. Pipes do not have edges at (a) and (b) in Figure 2. To utilise the SAFT algorithm it is necessary to introduce a periodic boundary condition at these edges and consider this boundary for calculation of the beeline between transmitter, image point and receiver.

3. SIMULATION OF GUIDED ELASTIC WAVES

3.1 Simulation Model

A common method for solving elastic, time-dependent problems is the finite-difference method which is often used for simulating ultrasonic guided elastic waves as Fromme [9] or Balasubramanyam [10] reported. In this paper a full three dimensional model is simulated with the software Wave3000Plus. To reduce computing time, the pipe with a diameter of 193,7 mm and a wall thickness of 10 mm is unwrapped to a plate with a width of 608,5 mm and a length of 1500 mm. Regarding to Rose [5] it is possible to unroll the pipe and regard it as an isotropic plate if the diameter is much larger than the wall thickness. Thereby the solution of the fundamental SH0-mode in a plate corresponds to the T(0,1)-mode in pipes, while the solution of the fundamental A0-mode in a plate corresponds to the L(0,1)-mode in pipes. However, in order to treat an unwrapped pipe as a plate, an extra boundary condition has to be considered. In addition to the traction free boundary condition at the top and bottom of the plate, a boundary condition occurs along the axial cut. The solution of one edge of the plate has to match the other edge in order to remove the discontinuity by unrolling the pipe. The remaining edges were constrained with infinite or perfectly matched layer boundary conditions whereby incoming waves were absorbed and not reflected back into the plate. Figure 3 shows the size of the simulation model, the position of transducers and the analogy between pipe and plate.

The plate is made of a S355 mild steel ($E = 210,56 \text{ GPa}$, $\nu = 0,3$) as it is often used for offshore applications. A v-shaped seam with an opening angle of 50° , an acceptable weld upset of 2,5 mm and a weld reinforcement of 0,75 mm is located in the centre of the plate. Compared to the surrounding material, the material parameter of the seam has a variation of 4%. Twelve transducers are located in a distance of 250 mm from the lower edge and were positioned equally spaced along the plate. Excitation in vertical direction (out-of-plane) is applied to each single transducer which will lead to pure excitations of lamb waves. Subsequently, the transducers will receive displacements in vertical and horizontal direction.

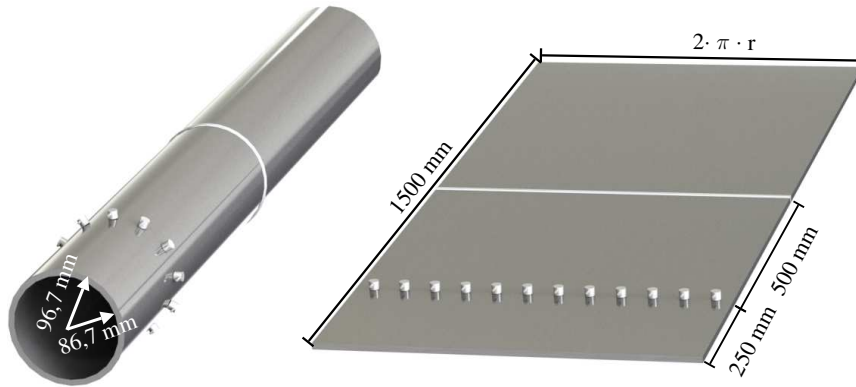


Figure 3 : Geometry of unwrapped pipe

3.2 Simulation Results

As a first step the model was validated regarding the analytical solution of the wave equation. Therefore the convergence of the time signals were determined. It became apparent that at least 18 points per wavelength are necessary to minimize the influence of numerical dispersion. The occurrent error in wavespeed is less than 1 % compared to the analytical dispersion curve. For every presented wave mode at any given frequency at least 20 points per wavelength were provided.

Consecutively, the interaction of excited guided wave with a crack growing in direction of the wall thickness was investigated. The crack had a length of 20 mm, a width of 1 mm and a varying depth between 1 and 10 mm. It was located in a distance of 500 mm from the transducers in parallel to the weld seam. While activating all transducers at the same time, a plane lamb wave was excited in the plate. By presetting only vertical displacements for excitation, the asymmetric wave modes A0 and A1 ($\sim L(0,1)$ and $L(0,3)$ in the observed frequency range) were primarily excited. The distance between transducers and crack yields to a separation of excited wave modes at any excited frequency in time domain. Interactions between crack and lamb wave modes will be assessed by a damage index based on Park [6] which is defined as

$$DI_{RMSD} = \sqrt{\frac{\sum_{i=1}^N (y_i - x_i)^2}{\sum_{i=1}^N x_i^2}} \cdot 100, \tag{2}$$

where x_i and y_i are time signals of the intact and damaged state on the same signal path at discrete sample points i . This damage index describes the change of the signal energy between two states in percent. Figure 4 shows the trend of the damage index by discrete frequencies for the A0 lamb wave mode. The trend shows an average value of the damage index for all twelve transducers and a symmetry regarding the middle of the plate. The trend increases until the crack achieves a depth of 4 mm. Between 4 and 6 mm, no significant changes in damage index can be observed, while the damage index increases when the crack grows deeper than 6 mm to the full wall thickness. The trend of the damage index results from principal trend of the stress component responsible for the crack interaction. Guided wave modes in the simulation model show a strong interaction with cracks perpendicular to the propagation direction if they have high normal stress components σ_x or shear stress components τ_{xy} or τ_{xz} . Both asymmetric wave modes A0 and A1 have high normal stress ratios σ_x that refer to an interaction and a scatter field at the crack. Close to the upper and lower surface of the plate, a maximum of normal stress for asymmetric wave mode appears which leads to an increase of the damage index. At the middle of the plate between 4 and 6 mm appears a minimum of normal stress. The incident wave does not interact with the crack in this region which cause almost no change in damage index. An equivalent behaviour is reported by Demma [2] who studied the reflection of

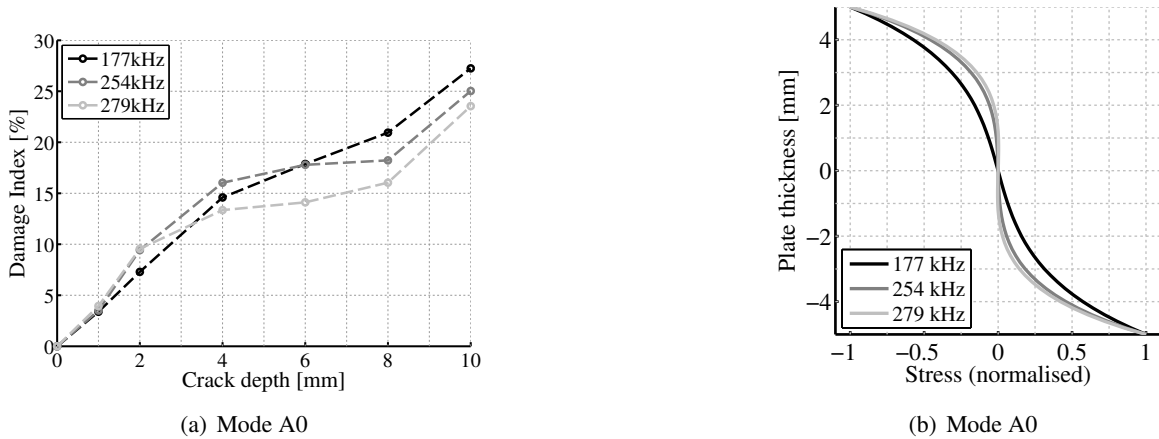


Figure 4 : Trend of damage index (left) and mode shape of stress component σ_x (right) of A0 wave mode at different frequencies [8]

cracks growing in direction of wall thickness with the fundamental shear wave mode T(0,1). Demma reported a linear relationship between crack depth and reflection coefficient. Due to a constant trend of shear stress τ_{xy} , the reflection coefficient will increase linear with crack depth. Figure 5 shows the reconstruction of the simulated crack with the SAFT algorithm at a frequency of 330 kHz. The image is displayed as an unwrapped pipe, the vertical axis denotes the unwrapped length whereas the horizontal axis denotes the axial position according to the actuators (gray circles). The reconstruction in Figure 5(a) was carried out with the A0 wave mode. The image shows the crack at the correct location at $X = 0,5$ m and $Y = 0,305$ m with an amplitude of 3,6. In the dispersion diagram it can be seen that the A1 wave mode has a higher wave velocity and a reflection will occur earlier in time signal. In the reconstruction the crack can be identified at $X = 0,415$ m and $Y = 0,305$ m with a significant lower amplitude. Because of a lower excitation of the A1 wave mode the difference amplitudes will have a lower energy level. Figure 5(b) shows the reconstruction with the A1 wave mode. To obtain the image, the time signal was truncated after the A1 mode has passed to reduce the influence of other wave modes. In comparison to the A0 wave mode, the defect amplitude of the reflected signal is reduced by 40 %.

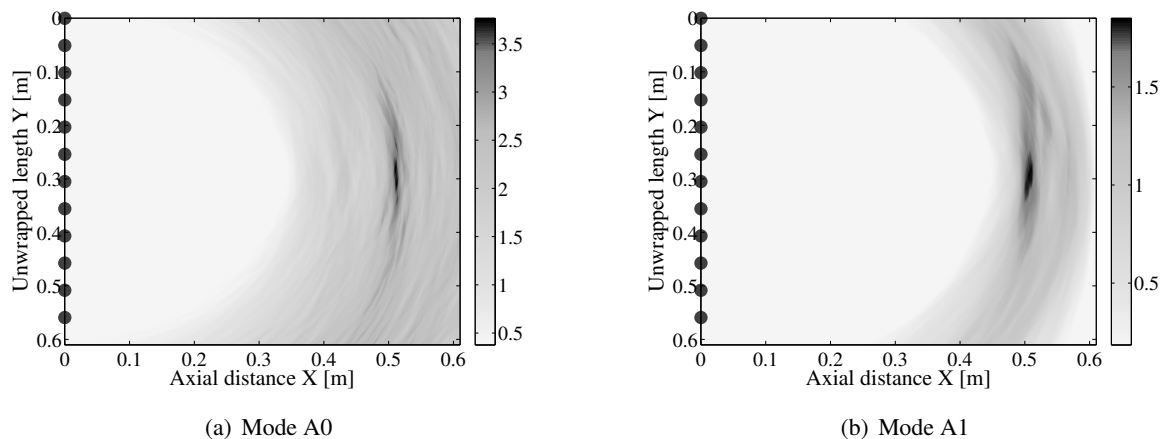


Figure 5 : Reconstructed SAFT images of A0 (a) and A1 (b) using simulation data of a 1 mm depth crack at an axial position of 0,5 m and a circumferential position of 0,305 m [8]

4. EXPERIMENTAL WORK ON LABORATORY DEMONSTRATOR

4.1 Experimental Setup

The measurements were carried out on a scaled laboratory demonstrator. Depending on the simulation model, the laboratory demonstrator consisted of mild steel pipe with a diameter of 193,7 mm and a wall thickness of 10 mm. The appropriate pipe had a length of 3000 mm. In comparison to a real offshore structure, the used pipe had a smaller diameter which was reduced by a multiplier of 3,9. At the same time the wall thickness was reduced by a multiplier of 2,5. To transfer the results of the laboratory demonstrator to a real offshore structure, it is necessary to adapt the test frequency. As the wave velocity is a function of the wall thickness and the frequency, it is possible to adjust the same behaviour of guided waves in a smaller structure if the test frequency is increased. The examined frequency domain is shown in Figure 1.

A transducer ring with twelve equally spaced piezoelectric disks of type FPM220 was sending and receiving longitudinal wave modes $L(0,1)$ and $L(0,3)$. The transducer ring is in a distance of 1 m of the left pipe end and 0,5 m from the weld seam. In this configuration, the reflection from the back wall do not interfere with the signal itself. The notch was located in the middle of the pipe and was enlarged stepwise between a depth of 1 and 4 mm starting at the outer surface of the pipe. In addition, the notch had a circumferential extend of 20 mm. A Multi-Channel-Acoustic-System (MAS) was used for ultrasonic signal generation and a digital oscilloscope LDS Nicolet Genesis 7t was utilized for signal recording. A PC controlled the complete measurement chain and conducted signal processing retrospectively. The entire measurement setup is shown in Figure 6.

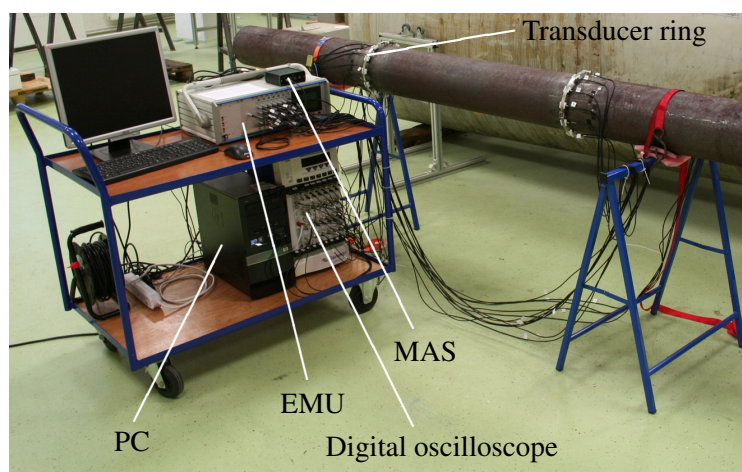


Figure 6 : Utilized measurement setup with transducer ring, MAS, oscilloscope and PC [8]

4.2 Experimental Results

The first step was the determination of the actual state of the pipe which was used as baseline data. Guided waves were excited at discrete frequencies from 177 to 330 kHz by the MAS. This corresponds to frequencies between 70 and 130 kHz in the unscaled pipe. After the baseline data were acquired the notch was enlarged in three steps. After every step the state of the pipe was measured and saved to the PC. To minimize signal noise, every signal path was measured one hundred times. All additional steps for signal processing like averaging, filtering, signal correlation, difference between damaged and undamaged state and image reconstruction were carried out in the MATLAB environment afterwards. Figure 7 shows the reconstructions for notches with a depth of 1 mm and 4 mm at a frequency of 279 kHz. In addition Table 1 presents the coordinates of the reconstructed notches and the relative

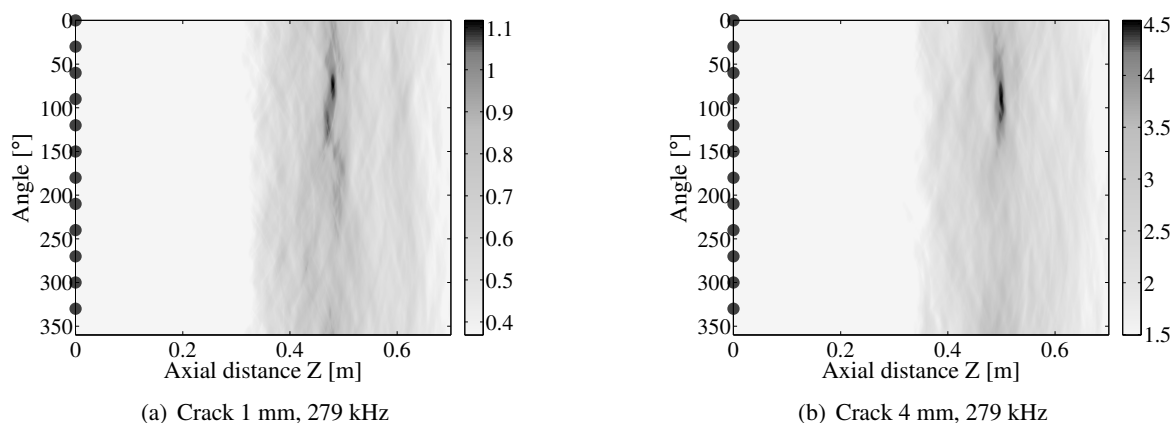


Figure 7 : Reconstructed SAFT images of a 1 mm depth notch (a) and a 4 mm depth notch (b) using the L(0,1) wave mode; real notch at an axial position of 0,5 m and an angle of 88° [8]

image error to an ideal reconstruction at different frequencies. At the presented frequencies, the circumferential position of the notch is mapped with a high accuracy compared to the accurate position. In axial direction, the accurate and the reconstructed notch position differs by up to 2 cm. An ideal reconstruction is obtained at a frequency of 279 kHz when the notch depth extend 1 mm. The reconstructed notch position and their relative error are shown in Table 1. The relative image error was calculated by

$$f = \frac{\|M_{opt} - M\|}{\|M_{opt}\|} \tag{3}$$

where M is the reconstructed image and M_{opt} is the ideal reconstructed image with almost no image noise. With increasing notch depth, the image noise is reduced which leads to a decreasing relative image error and a better notch identification. The lowest relative image error was determined for the reconstructions with 279 kHz. This can be explained by differences in propagation velocities between the L(0,1) and L(0,3) wave modes. At 279 kHz, the difference in wave velocity equals 600 m/s which lead to a better separation of the modes in the signals. However, at 177 kHz exists only a slight difference in wave speed and both modes will not be separated at the transducers. In this case, the propagating wave fields can interfere with each other and the notch will be reconstructed displaced from the real location. Additionally, the wave field not used for image reconstruction will appear as image noise.

5. DISCUSSION

The conducted simulations show a non-linear behaviour between reflection coefficient and crack depth caused by the interaction of the asymmetric wave modes with the growing cracks in the direction of the wall thickness. The trend of the damage index agreed well with the stress component that mainly interact with the crack. For cracks with a depth of 1 mm, a deviation of signal energy of 2 to 5 % in dependence of wave mode and frequency was observed. In the investigated frequency range, cracks

Table 1 : Position and relative image error of reconstructed notches at elected frequencies

Frequency	Notch depth	Axial Position	Angle	Image error
177 kHz	1 mm	0,502 m	87°	9,8 %
177 kHz	4 mm	0,497 m	63°	8,3 %
279 kHz	1 mm	0,480 m	77°	9,1 %
279 kHz	4 mm	0,500 m	92°	7,6 %

with a depth fewer half the wall thickness showed an almost linear behaviour between crack depth and wall thickness. This relation could also be found also in measurement results. The damage amplitude for the L(0,1) wave mode in the reconstructed SAFT image showed an almost linear increase. In contrast to simulation by the SAFT algorithm, higher image noise occur in the measurements shown by the relative image error. In simulations, only multi mode behaviour of guided waves lead to image noise whereas in practical measurements instrumentation becomes apparent. Additionally, variable coupling conditions and variations in temperature lead to another measurement noise component. This measurement noise was determined in the experiments with 3 to 5 % of the maximum signal amplitude. This range covers the expected signal deviation due to the damage in case of a crack with a depth of 1 mm and has an additional impact on reconstruction accuracy.

6. SUMMARY AND OUTLOOK

The experiments were carried out in labscale and compared to simulation results. As it can be seen, the reconstruction of the artificially introduced crack to a pipe was successfully carried out. Nevertheless, it could also be proofed that the selection of the frequency has a significant impact on the detectability of defaults. Therefore, simulation are always helpful to predict the probability of detection with certain experimental parameters. The signals was processed and the root mean square of difference signal was used as damage indicator. The potential of the applied algorithm lies especially in the monitoring of pipes and welded seams to provide a safe and secure operation. Future works should aim for a failure catalogue to select the sensitive parameters more easily. Furthermore, the sensor rings will be equipped with other sensor types to detect also other modes for a broader application possibility.

ACKNOWLEDGEMENTS

The authors kindly thank the German Federal Ministry of Research and Technology for the funding and the Project Management Jülich for the support of the project UnderwaterInspect.

REFERENCES

- [1] A. Løvstad and P. Cawley. The reflection of the fundamental torsional guided wave from multiple circular holes in pipes. *{NDT} & E International*, 44(7):553 – 562, 2011.
- [2] A. Demma, P. Cawley, M. Lowe, A.G. Roosenbrand, and B. Pavlakovic. The reflection of guided waves from notches in pipes: a guide for interpreting corrosion measurements. *{NDT} & E International*, 37(3):167 – 180, 2004.
- [3] J.O. Davies and P. Cawley. The application of synthetic focusing for imaging crack-like defects in pipelines using guided waves. *IEEE Trans Ultrason Ferroelectr Freq Control*, 56(4):759–771, 2009.
- [4] L. Schubert, R. Schwerz, M. Leibowitz, U. Lieske, and B. Frankenstein. Guided wave based shm approach using saft-algorithm for impact detection in composite materials. *International Workshop on Structural Health Monitoring*, 8:1948–1955, 2011.
- [5] L. Li and J. L. Rose. Natural beam focusing of non-axisymmetric guided waves in large-diameter pipes. *Ultrasonics*, 44(1):35 – 45, 2006.
- [6] S. Park, Yun, Y. C.-B., Roh, and Y.-J. Lee. Pzt-based active damage detection techniques for steel bridge components. *Smart Materials and Structures*, 15(4):957, 2006.
- [7] J.-W. Kim, C. Lee, and S. Park. Real-time health monitoring of pipeline structures using piezoelectric guided wave propagation. *Advanced Science Letters*, 4(3):696–701, 2011.
- [8] T. Gaul. Anpassung des SAFT-Verfahrens zur Fehlererkennung an metallischen Offshore-Gründungsstrukturen. Master's thesis, Technische Universität Dresden, 2013.
- [9] P. Fromme and M. B. Sayir. Detection of cracks at rivet holes using guided waves. *Ultrasonics*, 40(18):199 – 203, 2002.
- [10] R. Balasubramanyam, D. Quinney, R. E. Challis, and C. P. D. Todd. A finite-difference simulation of ultrasonic lamb waves in metal sheets with experimental verification. *Journal of Physics D: Applied Physics*, 29(1):147–155, 1996.